

**Driving a dissipative quantum oscillator**

P. C. López Vázquez

*Departamento de Ciencias Naturales y Exactas, Universidad de Guadalajara, Carretera Guadalajara, Ameca Km. 45.5, C.P. 46600, Ameca, Jalisco, Mexico*

(Received 26 June 2018; published 24 October 2018)

The open driven quantum harmonic oscillator is studied for three different possible mechanisms of driving; a generalization of the forced oscillator, driving due to a time-dependent coupling to a two-level system, and driving due to an adiabatic modulation of the frequency. The first case encompasses all possible configurations going from the standard forced harmonic oscillator to the classical pumping type of driving typically used in quantum optics. In the second case, an additional two-level system, coupled to the oscillator at a time-varying rate, is assumed and the reduced dynamics of the oscillator and the qubit is examined. In the driving due to adiabatic modulation, the dynamics of a harmonic oscillator whose frequency slowly varies in time is studied. The study done in this paper is focused on a harmonic type of driving, although the solutions are derived for an arbitrary type of driving. In all the cases, the oscillator is assumed to be in contact with a zero- or finite-temperature environment, which provides dissipation to the system. The treatment done in this paper is fully analytic and the derivation of the solutions is based on the employment of the double Fourier transform of the Wigner function.

DOI: [10.1103/PhysRevA.98.042128](https://doi.org/10.1103/PhysRevA.98.042128)**I. INTRODUCTION**

The topic of quantum thermodynamics has drawn a great deal of attention in recent years, mostly due to the questions and the implications it places on the quantum scene by extending the ideas of the classical concepts such as work, heat, entropy, and thermalization to the microscopic quantum systems [1–6]. A large number of studies have been focused on the energy conversion issues and the extraction of work from thermal quantum machines, for which certain idealizations of quantum thermodynamic cycles and quantum heat machines have been proposed, e.g., [7–12]. The conception of quantum thermal machines relies on the possibility of an accurate manipulation of nonequilibrium dynamics and particularly the application of driving into the quantum states, which by nature are open, plays a fundamental role [13–18]. Besides the implications of the driven dynamics in quantum thermodynamics, quantum systems which are subject to the interaction of time-dependent external fields have become fundamental in many areas of quantum physics such as quantum chemistry and quantum optics [19]. In particular, the manipulation of the populations in atoms and molecules is one of the fundamental mechanisms needed to achieve quantum computation [20]. External driving has also been used to study synchronization [21–25] and the modulation of the energy levels [26], where the transition frequencies are time dependent and also strongly driven systems have reported the formation of dressed states and enhanced decoherence [27–29], although it has been said that driving alone can be used as a dissipative mechanism [30]. A key point in all these approximations is the influence an external environment has on the quantum system for which open quantum dynamics should be always assumed [31]. In fact, the possibility of generating novel quantum states emerging out of the nonequilibrium dissipative dynamics is also an interesting topic [32,33].

This paper will deal with various models of driving exerted on a quantum harmonic oscillator in contact with a thermal reservoir, aiming to provide a full understanding of the effects of driving and dissipation and to show certain interesting dynamical regimes happening for certain parameters. The types of driving that will be studied in this paper are (a) driving exerted due to external time-dependent forces, which encompasses a certain range of drivings going from the standard forced harmonic oscillator to the classical pumping type of driving that a mode of a quantum field inside a cavity would experience; (b) driving imposed on an oscillator due to a time-dependent coupling with an additional two-level system [34], which could in principle be observed in superconducting quantum devices such as Cooper pair boxes [35], flux qubits [36], or Josephson junctions [37,38]; and (c) driving due to an adiabatic modulation of the transition frequency of the oscillator [26,39]. In all these cases, it is also assumed that the oscillator is in contact with a thermal reservoir which produces dissipation and thermalization and the open dynamics of the system is described by means of a master equation. The type of environment is modeled within the framework of the Lindblad master equations for the finite zero-temperature environmental model. It should be mentioned that the analysis done here is fully analytic and the derivation of the solutions is done in the framework of the double Fourier transform of the Wigner function, or chord function, as it has been called [40,41]. The paper is organized as follows. In Sec. II, a description of the driving mechanisms and the model of dissipation that will be treated in this paper are given, together with a brief description of the chord function which will be used to derive the analytical solutions. In Sec. III, the analytical solutions of a generalization of a forced oscillator are studied for different driving and bath parameters. In Sec. IV, the case of a time-varying coupling

of the oscillator to a qubit is studied, focusing on the reduced dynamics for the oscillator and the qubit. In Sec. V, the case of a time-dependent transition frequency at the adiabatic limit is studied. In Sec. VI, a summary of the results is given.

## II. MECHANISM OF DRIVING AND DISSIPATION

Three different models of driving will be studied in this paper: the driving due to the action of external time-dependent forces, the driving due to the time-dependent interaction with a qubit, and the driving caused by a modulation of the transition frequency of the oscillator. These models of driving will be applied to a harmonic oscillator whose Hamiltonian, described in a dimensionless framework, is given by

$$H_{\text{osc}} = \frac{\hat{x}^2}{2} + \frac{\hat{p}^2}{2}, \quad (1)$$

where in the dimensionless description  $\hat{X} = \sqrt{\hbar/m\omega_0}\hat{x}$  and  $\hat{P} = \sqrt{\hbar m\omega_0}\hat{p}$ , with  $\hat{X}$  and  $\hat{P}$  the position and momentum operators, respectively, and  $\omega_0$  the angular frequency of the oscillator; all the dynamics will be measured in the dimensionless timescale  $\tau = \omega_0 t$ . In the following, a brief description of these types of driving mechanisms is given.

The driving exerted due to an external time-dependent force can be more generally described in the context of the driving that a mode of a quantum field inside a cavity will experience (the cavity will later be considered to have losses and thermal photons) when it is pumped by a classical force [42]. Formally, the Hamiltonian for the driving is expressed as  $H_d(\tau) = \alpha(\tau)\hat{a} + \alpha^*(\tau)\hat{a}^\dagger$ , and if  $\alpha(\tau)$  is a real function, then the system becomes the type of driving of a forced oscillator, i.e.,  $H_d(\tau) = f(\tau)\hat{x}$ , with  $f(\tau) = \sqrt{2}\alpha(\tau)$ . With the aim of giving a deeper study of the dynamics with this type of driving, one can write the creation and annihilation operators in terms of the position and momentum operators

$$H_d(\tau) = f(\tau)\hat{x} + g(\tau)\hat{p} \quad (2)$$

and keep the time-dependent functions  $f(\tau)$  and  $g(\tau)$  unspecified, since the general solution can be obtained without an explicit description of these functions. One can see that the case when  $f(\tau) = \sqrt{2}\text{Re}[\alpha(\tau)]$  and  $g(\tau) = -\sqrt{2}\text{Im}[\alpha(\tau)]$  corresponds to the case of driving due to a classical pumping and in the case when  $g(\tau) = 0$  one recovers the case of the force oscillator.

One additional possible way to introduce driving to the oscillator is in the context of composite qubit-oscillator systems, considering a time-dependent coupling to a two-level system via dephasing coupling (e.g.,  $\sigma_z \otimes \hat{x}$ ). These type of realizations could in principle be realizable in superconducting qubit-oscillator devices [34,43–45], where one could in principle engineer a time-varying interaction. Nevertheless, in order to comprise a bigger class of induced driving, one can adopt a more general type of dephasing coupling through the position and the momentum as well. In the dimensionless description frame described above, the Hamiltonian of the composite system will have the form  $H(\tau) = H_q + H_{\text{osc}} + H_d(\tau)$ , where

$$H_d(\tau) = \sigma_z \otimes [f(\tau)\hat{x} + g(\tau)\hat{p}], \quad (3)$$

$H_q = -\Delta\sigma_z$  is the Hamiltonian of the qubit, and  $\sigma_z$  is the  $z$  component of the Pauli matrices.

The last type of driving corresponds to an adiabatic modulation of the frequency of the oscillator. The Hamiltonian for this driving may be written as

$$H_d = \frac{1}{2}f(\tau)\hat{x}^2 \quad (4)$$

such that the total Hamiltonian of the system may be written as  $H(\tau) = H_{\text{osc}} + H_d(\tau) = \hat{p}^2/2 + \Omega^2(\tau)\hat{x}^2/2$ , where  $\Omega^2(\tau) = 1 + f(\tau)$ . As before,  $f(\tau)$  remains an arbitrary time-dependent function which does not need to be specified to obtain a solution; it only needs to fulfill the adiabatic condition, which in this case reads  $|\dot{\Omega}(\tau)/\Omega(\tau)| \ll \gamma$ , with  $\gamma$  characterizing the coupling rate to the thermal environment. For all these types of drivings, we will also be considering that the oscillator is additionally interacting with a thermal environment which dissipates the dynamics of the oscillator. In the following, a brief description of the dissipative mechanism that will be contemplated is given.

### A. Master equations

The dynamics of an open system is generally described through a master equation of the reduced system which consists of two parts: the von Neumann dynamics where the unitary dynamics is contained and the dissipative dynamics due to the interaction with the environment. In the dimensionless description frame referred to above, the master equation for each of the referred systems described before will have the form

$$i\frac{d\rho}{d\tau} = [H(\tau), \rho] + i\mathcal{L}[\rho], \quad (5)$$

where  $H(\tau)$  refers to each of the total Hamiltonians of the driven systems, while the superoperator  $\mathcal{L}[\rho]$  describes the nonunitary dissipative part of the dynamics. In this paper, the model of dissipation that will be used is the finite zero-temperature model, based on the quantum optical type of interaction and whose dissipator has a Lindblad form [31]

$$\mathcal{L}[\rho] = -\gamma(\bar{n} + 1)\mathcal{D}[\hat{a}\rho] - \gamma\bar{n}\mathcal{D}[\hat{a}^\dagger\rho], \quad (6)$$

where  $\mathcal{D}[\cdot]$  is defined through  $\mathcal{D}[\hat{A}\hat{B}] = \{\hat{A}^\dagger\hat{A}, \hat{B}\} - 2\hat{A}\hat{B}\hat{A}^\dagger$  and  $\bar{n} = (e^{1/D} - 1)^{-1}$  is the average number of excitations of the harmonic oscillator at thermal equilibrium;  $D = k_B T/\hbar\omega_0$  is the dimensionless diffusion constant and  $\gamma = \gamma_0/\omega_0$  is the dimensionless damping rate or coupling rate to the environment. Nevertheless, approximations based on a high-temperature environmental model such as the Caldeira-Leggett model can be derived by following similar steps [46,47]. Particularly useful in solving the dynamics of the open oscillator is the employment of the Fourier transform of the Wigner function, sometimes called the chord function [40,41], since the solutions of the master equations can be easily integrated by the application of the fundamental matrix of the damped motion which emerges naturally under this description. In the following, a brief description of the properties of the chord function is given.

### B. Chord function

In the literature, one can find different ways to solve or approximately solve the master equations. One particular way to do so is by employing the Fourier transform of the Wigner

function, also called the chord function [40,41], or characteristic function, in quantum optics [48], which is defined in the following way:

$$w(k, s; \tau) = \int_{-\infty}^{\infty} \int_{-\infty}^{\infty} dp dq e^{ikq+isp} W(q, p; \tau) \quad (7)$$

$$= \int_{-\infty}^{\infty} dq e^{ikq} \langle q + s/2 | \varrho(\tau) | q - s/2 \rangle. \quad (8)$$

In this description, the evolution of observables can be obtained by setting  $\langle \hat{A}(\tau) \rangle = \int_{-\infty}^{\infty} \int_{-\infty}^{\infty} d\vec{r} w(\vec{r}, \tau) \hat{A}(\vec{r})$ , where  $\hat{A}(\vec{r})$  is the Fourier transform of the Weyl symbol of operator  $\hat{A}$  [42,49]. In particular, the first and second moments can be easily obtained from the chord function solutions as  $\langle \hat{x}^n \rangle = (-i)^n \partial_k^n w|_{k,s=0}$  and  $\langle \hat{p}^n \rangle = (-i)^n \partial_s^n w|_{k,s=0}$  for  $n = 1, 2$  and the first-order correlations are computed as  $\langle \hat{x} \hat{p} \rangle = -(\partial_{ks} - i/2)w|_{k,s=0}$  and  $\langle \hat{p} \hat{x} \rangle = \langle \hat{x} \hat{p} \rangle^*$ . The energy of the oscillator may be therefore calculated as

$$\begin{aligned} E(\tau) &= \frac{\langle \hat{p}^2 \rangle + \langle \hat{x}^2 \rangle}{2} \\ &= -\frac{1}{2} (\partial_k^2 + \partial_s^2) w(k, s, \tau) |_{k=0, s=0}. \end{aligned} \quad (9)$$

Additionally, the position and momentum probabilities distributions can be easily obtained as  $P(q, \tau) = \int_{-\infty}^{\infty} dk w(k, 0) e^{-ikq}$  and  $P(p, \tau) = \int_{-\infty}^{\infty} ds w(0, s) e^{-isp}$ , respectively.

### III. DRIVING DUE TO AN EXTERNAL FORCE

The master equation for this type of driving described above will have the form

$$i \frac{d\varrho}{d\tau} = [H_{\text{osc}} + f(\tau)\hat{x} + g(\tau)\hat{p}, \varrho] + i\mathcal{L}[\varrho]. \quad (10)$$

In the chord function representation, the master equation becomes

$$\hat{L}w = -i[f(\tau)s - g(\tau)k]w, \quad (11)$$

where  $w = w(\vec{r}, \tau) = w(k, s, \tau)$  and  $\hat{L}$  is a linear differential operator whose explicit form is

$$\hat{L} = \partial_\tau + (s + \gamma k)\partial_k - (k - \gamma s)\partial_s + \frac{\gamma_+}{2}(k^2 + s^2), \quad (12)$$

with  $\gamma_+ = 2\gamma(\bar{n} + 1/2)$ . The solution for the master equation (11) is derived in Appendix A. It represents the evolution of the chord function from some initial time  $\tau_0$  to an arbitrary final time  $\tau_0 + \tau$  as given by

$$\begin{aligned} w(\vec{r}, \tau_0 + \tau) &= w[\mathbf{R}(-\tau)\vec{r}, \tau] \exp\left(-\frac{\gamma_+}{2}\alpha(\tau)|\vec{r}|^2\right) \\ &\quad \times \exp[-i\vec{\chi}(\tau_0 + \tau) \cdot \vec{r}], \end{aligned} \quad (13)$$

where the first line represents the solution for the coupling of the oscillator with the thermal reservoir alone and the second line corresponds to the action of the driving to the oscillator which is completely contained in the vector  $\vec{\chi}(\tau_0 + \tau)$ , appearing as an additional phase to the solution of the contact with the thermal bath. The term  $w[\mathbf{R}(-\tau)\vec{r}, \tau]$  is the initial condition of the oscillator, whose variable dependence has been mapped with the fundamental matrix

$\mathbf{R}(-\tau)$ . The fundamental matrix represents a rotation and a contraction-expansion map

$$\mathbf{R}(\tau) = e^{\gamma\tau} \begin{pmatrix} \cos \tau & \sin \tau \\ -\sin \tau & \cos \tau \end{pmatrix} \quad (14)$$

and possesses group properties in the sense that  $\mathbf{R}(\tau)\mathbf{R}(\tau') = \mathbf{R}(\tau + \tau')$  and  $\mathbf{R}^{-1}(\tau) = \mathbf{R}(-\tau)$ . Additionally, the function  $\alpha(\sigma)$  is given by

$$\alpha(\tau) = \int_0^\tau d\tau' [R_{11}^2(-\tau') + R_{12}^2(-\tau')] = \frac{1 - e^{-2\gamma\tau}}{2\gamma}. \quad (15)$$

As stated before, all the influence of the driving to the oscillator appears in the phases appearing in the second line of (13), where the components of the vector  $\vec{\chi}^T(\tau_0 + \tau) = [\chi_1(\tau_0 + \tau), \chi_2(\tau_0 + \tau)]$  are the convolution of the time-dependent forces with the matrix elements of the fundamental matrix, i.e.,

$$\chi_1(\tau) = (R_{21}^{-1} \star f)(\tau) - (R_{11}^{-1} \star g)(\tau), \quad (16)$$

$$\chi_2(\tau) = (R_{22}^{-1} \star f)(\tau) - (R_{12}^{-1} \star g)(\tau). \quad (17)$$

Probably a more traditional way to see the solutions is in terms of the Wigner function. This can be easily calculated by computing the double inverse Fourier transform of the solution (13), although to get the Wigner function description of the solution one must state first the initial conditions of the oscillator. Assuming a general coherent initial state  $\psi(x) = \exp[ip_0x - (x - x_0)^2/2]/(2\pi)^{1/4}$ , with  $x_0$  and  $p_0$  the initial average position and momentum of the oscillator, respectively, then the Wigner function reads

$$W(\vec{x}, \tau) = \frac{1}{2\sqrt{\det\mathbf{\Sigma}(\tau)}} e^{-[\vec{x} - \vec{x}_0(\tau)]^T \mathbf{\Sigma}(\tau)^{-1} [\vec{x} - \vec{x}_0(\tau)]/4}, \quad (18)$$

where the vectors have been defined in the phase space  $\vec{x} = (q, p)^T$  and  $\vec{x}_0(\sigma) = \mathbf{R}^T(-\tau)\vec{x}_0 - \vec{\chi}(\tau_0 + \tau)$ , with  $\vec{x}_0 = (x_0, p_0)^T$ , and  $\mathbf{\Sigma}(\tau)$  is a  $2 \times 2$  diagonal matrix whose components are given by  $\Sigma_{11}(\tau) = \Sigma_{22}(\tau) = e^{-2\gamma\tau}/4 + \gamma_+\alpha(\tau)/2$ . Thus, for an initial coherent state, the effect of the driving is only to drive the system along trajectories described by  $[R_{11}(-\tau)x_0 + R_{21}(-\tau)p_0 - \chi_1(\tau_0 + \tau), R_{12}(-\tau)x_0 + R_{22}(-\tau)p_0 - \chi_2(\tau_0 + \tau)]$ . This in turn implies that the effects of the bath and the driving are decoupled in the sense that the action of the bath is always directed to damp (throw the Gaussian packet to the origin) and thermalize (widen the Gaussian packet to a width equal to the temperature of the environment), while the driving moves the Gaussian packet along the trajectories described above. Therefore, the damping and the driving compete against each other, causing the system to find a nonequilibrium stationary condition. Furthermore, by using Eq. (9), one can calculate the energy of the oscillator

$$E(\tau) = E_0 e^{-2\gamma\tau} + (\bar{n} + \frac{1}{2})(1 - e^{-2\gamma\tau}) + \frac{1}{2} |\vec{\chi}(\tau_0 + \tau)|^2, \quad (19)$$

where  $E_0$  is the initial energy of the oscillator, the first two terms represent the transients of the energy in contact with the thermal environment alone and the last term is the contribution due to the driving.

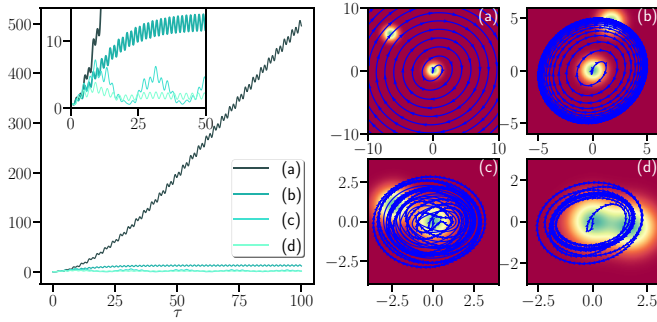


FIG. 1. Shown on the left is the time evolution of the dimensionless energy (vertical axis) and on the right the path in the dimensionless ( $q$ -horizontal axis,  $p$ -vertical axis) phase space of the Wigner function, for the resonant cases (a)  $\nu = 1$  and  $\gamma = 0.01$  and (b)  $\nu = 1$  and  $\gamma = 0.1$  and the out-of-resonance cases (c)  $\nu = 0.7$  and  $\gamma = 0.01$  and (d)  $\nu = 0.7$  and  $\gamma = 0.1$ , for the zero-temperature environmental model. On the right, the system, initially in the ground state, is represented by the coherent (Gaussian) state located at the origin. The driving moves the coherent state, keeping it coherent along the trajectories represented by the blue arrows. In these figures we have depicted the location of the coherent state after some time of evolution when it has move along the trajectory.

### Harmonic driving

Consider now a particular form of the time-dependent functions and let them be in a harmonic form  $f(\tau) = \lambda_1 \cos \nu_1 \tau$  and  $g(\tau) = \lambda_2 \sin \nu_2 \tau$  such that the forced oscillator case appears when  $\nu_2 = 0$ , while the classical pumping driving happens for  $\nu_1 = \nu_2$  and  $\lambda_1 = \lambda_2$ . In the former, the explicit form of the components of the vector  $\vec{\chi}$  is given in Eqs. (A14) and (A15). There one can see the appearance of resonances at  $\nu = 1$ . On the other hand, in the classical pump driving, the components of the vector  $\vec{\chi}$  are given in Eqs. (A16) and (A17) and for this case the resonance is suppressed. This fact has to do with equilibration of the rates of population and depopulation. Figures 1 and 2 depict, respectively, the zero-temperature limit and the finite temperature for an initial ground state of the oscillator for the forced oscillator, i.e.,  $\nu_2 = 0$ . The energy of the oscillator appears on the left and the arrowed blue lines on the right correspond to the trajectories the coherent state will follow for two values of the frequency of the driving (a resonant and a nonresonant frequency) and two values of damping. In the figures, one can observe that at small damping and resonant frequency [case (a)], the energy increases very rapidly and the Wigner function is driven out far from the origin. In case (b) the frequency of the driving is also at the resonant frequency but for a larger value of the damping and the system more rapidly reaches the nonequilibrium stationary condition described by a stationary orbit and an averaged quasistationary energy. For case (c) the frequency of the driving has been moved below the resonant frequency and uses a small damping. There one can observe that the coherent state is sometimes moved away from the origin and sometimes driven to the origin again, because for a driving out of resonance the driving could slow down or speed up the oscillator. When the damping is increased as seen in case (d), the system is taken into a nonequilibrium stationary condition, where the orbits have become dense. On the other

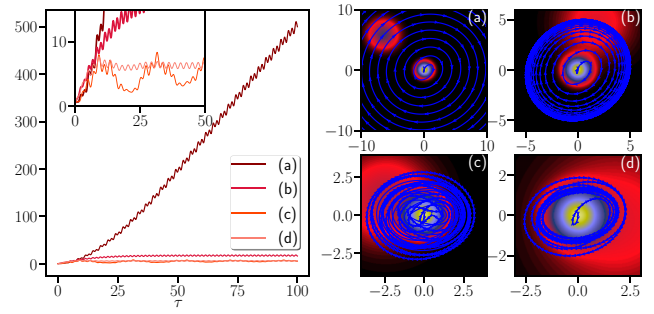


FIG. 2. Shown on the left is the time evolution of the dimensionless energy (vertical axis) and on the right the path in the dimensionless ( $q$ -horizontal axis,  $p$ -vertical axis) phase space of the Wigner function, for the resonant cases (a)  $\nu = 1$  and  $\gamma = 0.01$  and (b)  $\nu = 1$  and  $\gamma = 0.1$  and the out-of-resonance cases (c)  $\nu = 0.7$  and  $\gamma = 0.01$  and (d)  $\nu = 0.7$  and  $\gamma = 0.1$ . The temperature used was  $D = 5$ . On the right, the path that follows the initial coherent state located at the origin (the ground state) is represented by the blue curve. As the coherent state evolves in time it widens due to the influence of the temperature until it reaches a maximum width of the value of the temperature of the bath.

hand, Fig. 2 shows that the effect of the temperature is only to widen the Gaussian state until it reaches thermalization in the form of a Gibbs state. Figure 3 shows, for different values of the frequency of the driving, how the trajectories of the Wigner function will be affected when the damping (interaction strength of the environment) is increased.

Finally, Fig. 4 shows the dynamics of an initial cat state, under resonant driving ( $\nu_1 = 1$  and  $\nu_2 = 0$ ) with damping rate  $\gamma = 0.1$  and zero temperature. This case shows that the superposition pattern rapidly vanishes and the distance

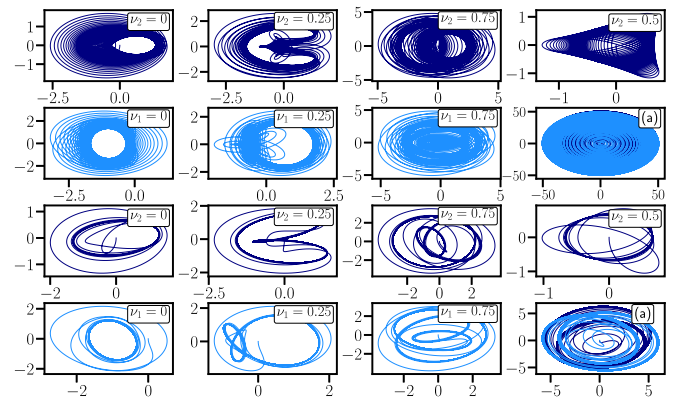


FIG. 3. Behavior of the trajectories of the Wigner function in the dimensionless ( $q$ -horizontal axis,  $p$ -vertical axis) phase space for an initial coherent state located at the origin (the ground state). The dark blue trajectories (dark lines) correspond to a fixed value of  $\nu_1 = 0.5$  while  $\nu_2$  changes; the light blue trajectories (lighter lines) correspond to a fixed value of  $\nu_2 = 0.5$  while  $\nu_1$  changes. The figures labeled with (a) correspond to the resonant cases  $\nu_1 = 0.5$  and  $\nu_2 = 1$  (dark blue curves) and  $\nu_2 = 0.5$  and  $\nu_1 = 1$  (light blue curves). In the top two rows the damping parameter is taken as  $\gamma = 0.01$  and in the bottom two rows it is taken as  $\gamma = 0.1$ . In all the trajectories the amplitudes of the driving are taken as  $\lambda_1 = \lambda_2 = \lambda = 1$ .

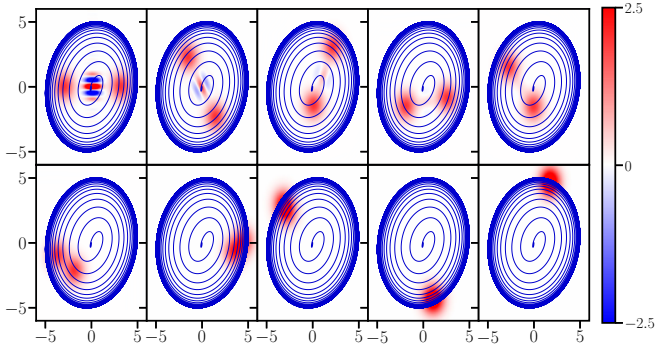


FIG. 4. Behavior of the trajectories of the Wigner function in the dimensionless ( $q$ -horizontal axis,  $p$ -vertical axis) phase space for an initial cat state at a resonant frequency of the driving,  $\nu_1 = 1$  and  $\nu_2 = 0$ , with an amplitude of  $\lambda_1 = 1$  and damping rate of  $\gamma = 0.1$  in the zero-temperature environmental model.

between the two Gaussians decreases, reaching a nonequilibrium stationary state in the form of a single coherent state following a stationary orbit exactly as in case (b) in Fig. 1. Also, one can observe that the center of the cat state follows the trajectory described by the vector  $\vec{\chi}(\tau_0 + \tau)$ .

#### IV. DRIVING DUE TO A VARYING INTERACTION WITH A QUBIT

One possible way to introduce driving to the dynamics of the oscillator is by coupling the oscillator, via a dephasing coupling, to a two-level system, with a time-varying coupling strength. For this setup, the master equation has the form

$$i \frac{d\varrho}{d\tau} = [H_q + H_{\text{osc}} + H_I, \varrho] + i\mathcal{L}[\varrho], \quad (20)$$

where

$$H_q = -\Delta\sigma_z \quad (21)$$

is the Hamiltonian of the qubit, with  $\sigma_z$  the  $z$  component of the Pauli matrices, and

$$H_I = \sigma_z \otimes [f(\tau)\hat{x} + g(\tau)\hat{p}], \quad (22)$$

with  $f(\tau)$  and  $g(\tau)$  describing the time-dependent coupling between the qubit and the oscillator. Now the density operator appearing in the master equation represents a reduced bipartite system consisting of the qubit and the oscillator  $\varrho \in \mathcal{H}_q \otimes \mathcal{H}_{\text{osc}}$ ; thus, by employing the notation  $\langle i|\varrho|j\rangle = \varrho_{ij}$  for  $i, j = 0, 1$  representing the projection of the system into the different states of the qubit, one gets a set of generalized master equations for the qubit matrix elements

$$i \frac{d\varrho_{00}}{d\tau} = [H_{\text{osc}}, \varrho_{00}] - [f(\tau)\hat{x} + g(\tau)\hat{p}, \varrho_{00}] + i\mathcal{L}[\varrho_{00}], \quad (23)$$

$$i \frac{d\varrho_{01}}{d\tau} = [H_{\text{osc}}, \varrho_{01}] - \{\Delta - f(\tau)\hat{x} - g(\tau)\hat{p}, \varrho_{01}\} + i\mathcal{L}[\varrho_{01}] \quad (24)$$

and the rest of the elements are obtained as  $\varrho_{11}(\tau) = 1 - \varrho_{00}(\tau)$  and  $\varrho_{10} = \varrho_{01}^*$ . In the chord function description, the generalized master equations becomes

$$\hat{L}w_{00} = -i[f(\tau)s - g(\tau)k]w_{00}, \quad (25)$$

$$\hat{L}_{\text{nd}}w_{01} = \left(i\Delta - \frac{\gamma_+}{2}(k^2 + s^2)\right)w_{01}, \quad (26)$$

where  $w_{ij} = w_{ij}(\vec{r}) = w(k, s, \tau)$ ,  $\hat{L}$  is defined in (12), and the nondiagonal element  $\hat{L}_{\text{nd}}$  is defined as

$$\hat{L}_{\text{nd}} = \partial_\tau + [s + \gamma k + 2f(\tau)]\partial_k - [k - \gamma s - 2g(\tau)]\partial_s. \quad (27)$$

It is not difficult to see that the differential equation for the diagonal element  $w_{00}$  has exactly the same form as that of the driven harmonic oscillator studied in the preceding section. Thus, for an initial decoupled system,  $\varrho(\tau_0) = \varrho_q(\tau) \otimes \varrho_{\text{osc}}(\tau)$  and then

$$w_{00}(\vec{r}, \tau_0 + \tau) = \varrho_{00}(\tau_0)w[\mathbf{R}(-\tau)\vec{r}, \tau_0] \times \exp\left(-\frac{\gamma_+}{2}\alpha(\tau)|\vec{r}|^2 - i\vec{\chi}(\tau_0 + \tau) \cdot \vec{r}\right), \quad (28)$$

where the components of the vector  $\vec{\chi}(\tau_0 + \tau)$  are defined in (16) and (17).

The derivation of the solution for the nondiagonal element is not as simple as in the diagonal case, but it can also be obtained exactly. The reader can review this derivation in Appendix B. The nondiagonal element has the form

$$w_{01}(\vec{r}, \tau_0 + \tau) = \varrho_{01}(\tau_0) \exp\left(i\Delta\tau - \frac{\gamma_+}{2}\Theta(\tau_0 + \tau)\right) \times w[\mathbf{R}(-\tau)[\vec{r} + \vec{\Lambda}(\tau_0 + \tau)] - \vec{\Lambda}(\tau_0), \tau_0] \times \exp\left[-\frac{\gamma_+}{2}[\alpha(\tau)|\vec{r}|^2 + 2\vec{\zeta}(\tau_0 + \tau) \cdot \vec{r}]\right], \quad (29)$$

where the vectors  $\vec{\Lambda}(\tau_0 + \tau)$  and  $\vec{\zeta}(\tau_0 + \tau)$  and the function  $\Theta(\tau_0 + \tau)$  are given in Eqs. (B12), (B18), and (B17), respectively.

#### A. Oscillator dynamics

Within these results, one would be interested in looking to the reduced dynamics of the oscillator or the qubit separately; to do so, one must perform a partial trace over one or the other degrees of freedom. The oscillator dynamics is obtained by performing a partial trace over the qubit, i.e.,  $w(\vec{r}, \tau_0 + \tau) = w_{00}(\vec{r}, \tau_0 + \tau) + w_{11}(\vec{r}, \tau_0 + \tau)$ , and then the reduced dynamics of the oscillator is described by the chord function

$$w(\vec{r}, \tau_0 + \tau) = w[\mathbf{R}(-\tau)\vec{r}, \tau_0] \exp\left(-\frac{\gamma_+}{2}\alpha(\tau)|\vec{r}|^2\right) \times [\varrho_{00}(\tau_0)e^{-i\vec{\chi}(\tau_0+\tau)\cdot\vec{r}} + \varrho_{11}(\tau_0)e^{i\vec{\chi}(\tau_0+\tau)\cdot\vec{r}}], \quad (30)$$

where  $\varrho_{00}(\tau_0)$  is the initial matrix element of the qubit. The solution corresponds to a linear combination of two oppositely driven oscillators. The Wigner function representing the dynamics of the oscillator can be easily calculated for

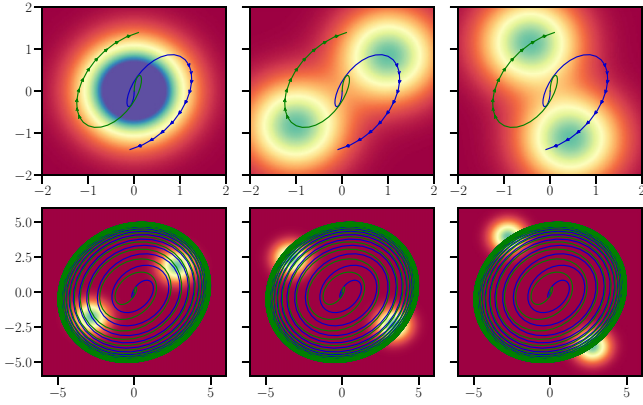


FIG. 5. Evolution of the Wigner function in the dimensionless ( $q$ -horizontal axis,  $p$ -vertical axis) phase space depicted at different stages of evolution, initially in the ground state, for the driving parameters  $\nu_1 = 1$ ,  $\nu_2 = 0$ , and  $\lambda_1 = 1$  and both parameters  $\gamma = 0.1$  and  $D = 0$ . For the case in which the temperature of the environment is different from zero, the situation is the same as described in Fig. 2 except the Gaussian states, which widen due to thermalization, are split into two.

an initial-state coherent state of the oscillator (in general, this conversion is straightforward for any Gaussian state, not only a coherent one), which corresponds to a linear combination of two Wigner functions in the form of (18), but moving in opposite directions, i.e.,

$$W(\vec{x}, \tau) = \varrho_{00}(\tau_0)W_-(\vec{x}, \tau) + \varrho_{11}(\tau_0)W_+(\vec{x}, \tau), \quad (31)$$

where  $\varrho_{00}(\tau_0)$  and  $\varrho_{11}(\tau_0)$  are the initial populations of the qubit states and

$$W_{\pm}(\vec{x}, \tau) = \frac{1}{2\sqrt{\det \Sigma(\tau)}} e^{-[\vec{x} - \vec{x}_0^{\pm}(\tau)]^T \Sigma(\tau)^{-1} [\vec{x} - \vec{x}_0^{\pm}(\tau)]/4}, \quad (32)$$

with  $\Sigma(\tau)$  being a  $2 \times 2$  diagonal matrix whose components are given by  $\Sigma_{11}(\tau) = \Sigma_{22}(\tau) = e^{-2\gamma\tau}/4 + \gamma_+\alpha(\tau)/2$  and  $\vec{x}_0^{\pm}(\tau) = \mathbf{R}^T(-\tau)\vec{x}_0 \pm \vec{\chi}(\tau_0 + \tau)$ . Therefore, the interaction with the qubit results in the splitting of the oscillator into two Gaussians, driven in opposite directions, through paths described by the convolution of the matrix elements of  $\mathbf{R}$  and the driven functions. Figure 5 exemplifies the dynamics of the oscillator in its Wigner function representation, when the coupling is assumed harmonic, i.e.,  $f(\tau) = \lambda_1 \cos \nu_1 \tau$  and  $g(\tau) = \lambda_2 \sin \nu_2 \tau$ , for a qubit initially in a superposition state  $|\psi\rangle = (|0\rangle + |1\rangle)/\sqrt{2}$  and the oscillator in its ground state. In contrast to the first scenario explored in Sec. II, where in the zero-temperature environmental model the system always remains coherent, now the oscillator becomes a mixture of two Gaussian states and the purity of the oscillator  $P_{\text{osc}}(\tau) = \frac{1}{2} \iint dp dq W^2(q, p, \tau)$  is related to the distance between the two Gaussians

$$P_{\text{osc}}(\tau) = \frac{\varrho_{00}^2(\tau_0) + \varrho_{11}^2(\tau_0)}{4\sqrt{\det \Sigma(\tau)}} + \frac{\varrho_{00}(\tau_0)\varrho_{11}(\tau_0)}{2\sqrt{\det \Sigma(\tau)}} \exp\left(\frac{-d^2(\tau_0 + \tau)}{2\sqrt{\det \Sigma(\tau)}}\right), \quad (33)$$

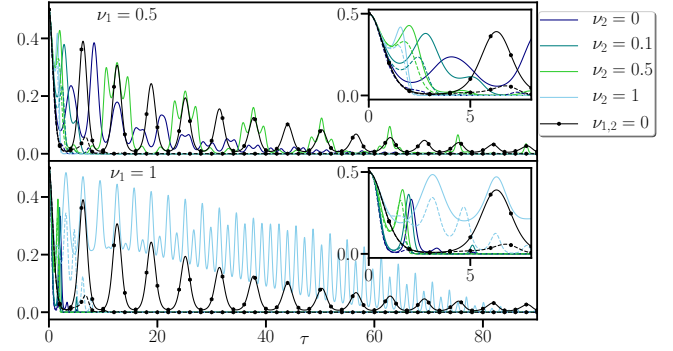


FIG. 6. Time evolution of the absolute value of the nondiagonal element of the qubit  $|\varrho_{01}(\tau)|$  (vertical axis) plotted for several values of the driving frequency with  $\lambda_1 = \lambda_2 = 1$  and for the zero-temperature environmental model. The solid lines correspond to  $\gamma = 0.01$  and the dashed lines to  $\gamma = 0.1$ . The black lines with circles correspond to the case when the coupling between the qubit and the oscillator is only through the position and the coupling strength is constant, i.e.,  $\sim \lambda \sigma_z \otimes \hat{x}$ .

where  $d(\tau_0 + \tau) = 2|\vec{\chi}(\tau_0 + \tau)|$  is the distance between the centers of the two Gaussians. Thus, if the two Gaussians become closer in the phase space, the oscillator recovers purity and vice versa.

## B. Qubit dynamics

The dynamics of the qubit are obtained by tracing out the oscillator degrees of freedom. This corresponds to evaluating the solutions (28) and (29) at  $\vec{r} = 0$ . For the diagonal elements, they keep their initial population steady, since this type of coupling does not involve transitions between the states. Nevertheless, the nondiagonal elements are strongly susceptible to the coupling to the oscillator. A nondiagonal element has the form

$$\begin{aligned} \varrho_{01}(\tau_0 + \tau) &= w_{01}(\vec{r}, \tau_0 + \tau)|_{\vec{r}=0} \\ &= \varrho_{01}(\tau_0)w[\mathbf{R}(-\tau)\vec{\Lambda}(\tau_0 + \tau) - \vec{\Lambda}(\tau_0), \tau_0]e^{i\Delta\tau} \\ &\quad \times \exp\left(-\frac{\gamma_+}{2}\Theta(\tau_0 + \tau)\right), \end{aligned} \quad (34)$$

where  $w(\cdot, \tau_0)$  represents the functional form of the oscillator in the chord function description at the initial time  $\tau_0$ , while  $\Theta(\tau_0 + \tau)$  and the vector  $\vec{\Lambda}(\tau_0 + \tau)$  are time-dependent functions given in Eq. (B17) and Eqs. (B7) and (B9), respectively. If the qubit does not have coherence at the initial time, no coherence will be generated at any time but, if the qubit is initially in a superposition state, then the nondiagonal terms will strongly depend on the coupling to the oscillator following the dynamics described by (34). Figure 6 plots the behavior of the nondiagonal element of the qubit as a function of time, for a harmonic coupling and for different values of the coupling frequency. In the figure, the black curves correspond to a standard-type non-time-dependent dephasing coupling, i.e.,  $\lambda \sigma_z \otimes \hat{x}$ . A remarkable thing to point out is that for the resonant case  $\nu_1 = n\nu_2 = 1$ , the dynamics of  $\varrho_{01}$  seems to be more resilient to the environmental effects than the dephasing coupling with constant coupling rate. This gain in the coherence could in principle be exploited as a method

of insulation of a qubit, through an engineered coupling to a resonator.

### V. ADIABATIC MODULATION

The derivation of a relatively simple analytical solution in the models treated so far relies deeply on the existence of a fundamental matrix for these types of dissipatively driven systems. In contrast, its construction is possible due to the integrability of the systems and their quadratic dependence on the dynamical variables. This in turn makes the shape of the Gaussian state inaccessible to the driving forces due to the decoupled effects of the thermalization and driving, i.e., the covariance matrix elements evolve only under the influence of the bath without noticing the effect of the driving and hence one may consider in a certain way that the types of driving exposed so far are trivial.

Nevertheless, one particular case of driving which affects the shape of a Gaussian state is the modulation of the distance of the energy levels, although for systems with time-dependent coefficients (the frequency of the oscillator in this case), the fundamental matrix may not be obtained in a closed analytical form [50,51] but only under certain approximations. In this section, the dynamics of such an open system is explored, in an adiabatic approximation. The master equation in this case corresponds to

$$i \frac{d\rho}{d\tau} = \frac{1}{2}[\hat{p}^2 + \Omega^2(\tau)\hat{x}^2, \rho] + i\mathcal{L}[\rho], \quad (35)$$

where  $\Omega^2(\tau) = 1 + f(\tau)$  and  $f(\tau)$  is a time-dependent function which varies very slowly with respect to the characteristic time evolution of the oscillator. This adiabatic change of the transition frequency opens the possibility to give an analytic solution for the dynamics with perceptible effects of the modulation, although certain restrictions must be assumed so that the solution may still be considered valid. The master equation in the chord function representation is

$$\{\partial_\tau + [\Omega^2(\tau)s + \gamma k]\partial_k - (k - \gamma s)\partial_s\} w = -\frac{\gamma_+}{2}|\vec{r}|^2 w, \quad (36)$$

where  $w = w(\vec{r}, \tau)$  and  $\vec{r} = (k, s)^T$ . The reader can consult Appendix C for the details of the derivation of the solution obtained under the adiabatic approximation, i.e.,  $|\dot{\Omega}/\Omega| \ll \gamma$ . This solution reads

$$w(\vec{r}, \tau_0 + \tau) = w[\mathbf{M}^{-1}(\tau_0 + \tau, \tau_0)\vec{r}, \tau_0] \times \exp\left(-\frac{\gamma_+}{2}\vec{r}^T \boldsymbol{\alpha}(\tau_0 + \tau)\vec{r}\right), \quad (37)$$

where now  $\mathbf{M}$  is the correspondent fundamental matrix in the adiabatic limit, having the form

$$\mathbf{M}(\tau_0 + \tau, \tau_0) = e^{\gamma\tau} \begin{pmatrix} \frac{\Omega(\tau_0 + \tau)}{\Omega(\tau_0)} \cos \omega(\tau) & \Omega(\tau_0 + \tau) \sin \omega(\tau) \\ -\frac{\sin \omega(\tau)}{\Omega(\tau_0)} & \cos \omega(\tau) \end{pmatrix}, \quad (38)$$

satisfying  $\mathbf{M}^{-1}(\tau_0 + \tau, \tau_0) = \mathbf{M}(\tau_0, \tau_0 + \tau)$ . We have also defined  $\omega(\tau) = \int_{\tau_0}^{\tau_0 + \tau} d\tau' \Omega(\tau')$ . The matrix  $\boldsymbol{\alpha}(\tau_0 + \tau, \tau_0)$  is

a symmetric matrix whose components are given by

$$\alpha_{ij}(\tau_0 + \tau) = \int_{\tau_0}^{\tau_0 + \tau} d\sigma' [\mathbf{M}(\sigma', \tau_0 + \tau) \mathbf{M}^T(\sigma', \tau_0 + \tau)]_{ij}. \quad (39)$$

For an initial coherent state as employed before, the Wigner function will have exactly the same form as given in (18) but now the components of the vector  $\vec{x}_0(\tau) = [x_0(\tau), p_0(\tau)]^T$  are the initial position and momentum of the oscillator, mapped with the transpose of the matrix  $\mathbf{M}^{-1}(\tau_0 + \tau, \tau_0)$ , i.e.,  $\vec{x}_0(\tau) = \mathbf{M}^T(\tau_0, \tau_0 + \tau)\vec{x}_0$ , with  $\vec{x}_0 = (x_0, p_0)^T$ . The covariance matrix  $\boldsymbol{\Sigma}$  is given by  $\boldsymbol{\Sigma}(\tau) = \frac{1}{4}\mathbf{M}^T(\tau_0, \tau_0 + \tau)\mathbf{M}(\tau_0, \tau_0 + \tau) + \gamma_+\boldsymbol{\alpha}(\tau_0 + \tau)/2$  and the energy can be obtained by using (9), yielding

$$E(\tau) = \frac{1}{2}\vec{x}_0^T \mathbf{M}(\tau_0, \tau_0 + \tau) \mathbf{M}^T(\tau_0, \tau_0 + \tau) \vec{x}_0 + \frac{1}{4}\text{Tr}\{\mathbf{M}(\tau_0, \tau_0 + \tau) \mathbf{M}^T(\tau_0, \tau_0 + \tau)\} + \frac{\gamma_+}{2}\text{Tr}\boldsymbol{\alpha}(\tau_0 + \tau). \quad (40)$$

These results have been derived without giving an explicit form of the modulating function  $f(\tau)$ , although it must fulfill the adiabatic condition. One way to choose the driving is in a harmonic form, i.e.,  $f(\tau) = \lambda \cos(\nu\tau)$ . For this type of modulation, the width of the harmonic potential will increase and decrease periodically with a period determined by the introduced dimensionless frequency  $\nu$ . For this particular choice of modulation, the adiabatic limit is determined within the condition  $|\lambda\nu \sin \nu\tau / (1 + \lambda \cos \nu\tau)| \ll 2\gamma$  and hence, for small values of damping, a complete period of the modulation would be very difficult to perceive, as very small modulation parameters are needed to keep the modulation in the adiabatic limit. On the other hand, for sufficiently large damping, one can employ larger values of the modulation parameters without reaching unjustified dynamics. Figure 7 shows the trajectories and the energies of a coherent state initially located at  $x_0 = 1$  and  $p_0 = 0$ , when the damping is increased for the zero-temperature and finite-temperature models of dissipation. The blue lines correspond to the analytical solutions under the adiabatic limit. These are contrasted with the trajectories and the energies of the numeric solutions of the dynamics without the adiabatic limit (black lines) and the dynamics of the oscillator without modulation (yellow lines). One can see that for short times (roughly one period of the oscillator without adiabatic modulation), the adiabatic approximation agrees well with the full numeric solution even for small damping rates. In the figure on the right, the wiggling of the energy is a consequence of measuring the energy with respect to a fixed frame of the oscillator without the adiabatic modulation, i.e.,  $E(\tau) = \langle \hat{p}^2 + \hat{x}^2 \rangle / 2$ . The evolution of the Gaussian coherent state for the zero-temperature and finite-temperature environmental models is given in Fig. 8 for a larger value of the modulating amplitude ( $\lambda = 0.5$ ) at a strong damping rate, so it is possible to perceive the effect of the modulation in the shape of the Gaussian packet. In this case, the Gaussian packet is deformed into a squeezed shape and this will happen periodically as the system evolves in time. The period of the maximum deformation will be fixed by the

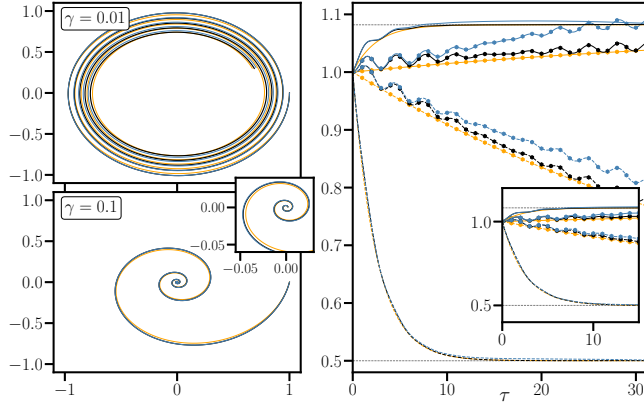


FIG. 7. Shown on the left are the trajectories in the dimensionless phase space ( $q$ -horizontal axis,  $p$ -vertical axis) of an initial coherent state located at  $q_0 = 1$  and  $p_0 = 0$  for two values of damping rates. On the right is the evolution of the energy (vertical axis) in its dimensionless description for zero temperature (dashed lines) and finite temperature (solid lines) and two values of damping,  $\gamma = 0.01$  (lines with markers) and  $\gamma = 0.1$  (lines without markers). The blue lines correspond to the adiabatic analytical solution of the model, the black lines (darker lines) correspond to the numeric full solution of the system without adiabatic approximation, and the yellow lines (lighter lines) correspond to the behavior of the system without any modulation. The modulation parameters taken here are  $\lambda = 0.05$  and  $\nu = 0.1$ .

modulation function. It should be pointed out that the adiabatic approximation carries with it a persistent error intrinsic in the derivation of the solution, a consequence of the assumptions needed in the approximations. The error increases as one approaches the adiabatic boundary, i.e.,  $\lambda\nu \sim \gamma$ , thus it becomes considerable for small damping regimes and large amplitude of the modulation and has its maximum value at times  $\tau = [n\pi - \arctan(\sqrt{1 - \lambda^2}/\lambda)]/\nu$  for  $n = 1, 2, \dots$ . Plotted in Fig. 9 is the evolution of the relative error as a function of the damping parameter of the standard deviations of the position [rows (a)] and momentum [rows (b)], the energy [rows (c)], and the uncertainty relation [rows (d)]. The brighter regions in the figure correspond to the regions of maximum error located around  $\tau = [\pi - \arctan(\sqrt{1 - \lambda^2}/\lambda)]/\nu$ , thus the interval where the error lies is settled by the frequency of the modulation while the amplitude of the modulation adjusts the position in this interval. Additionally, larger values of the damping make the error decrease. The noticeable stripes are identified with a shift in the frequency of the oscillator of the approximated solutions to its exact value.

### VI. SUMMARY

In this paper, the effects of different types of driving applied to a dissipative quantum oscillator have been studied, using analytical solutions derived for the models in the double Fourier transform of the Wigner function scenario. In particular, the study was done for harmonic-type driving applied to an initial coherent state of the oscillator, although

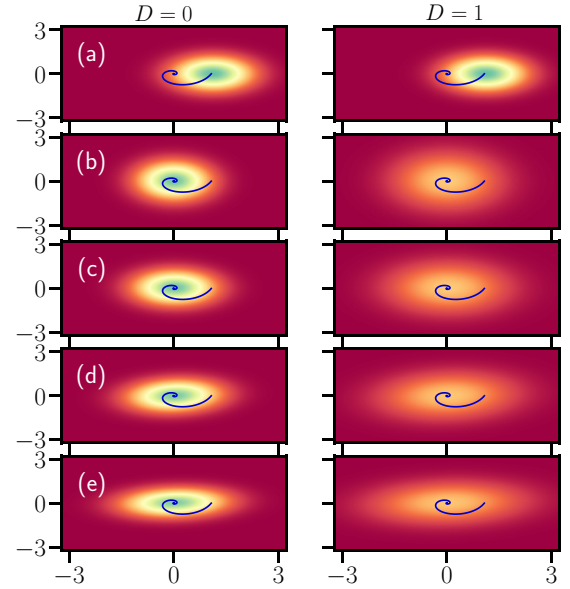


FIG. 8. Evolution of a Gaussian packet in the dimensionless phase space ( $q$ -horizontal axis,  $p$ -vertical axis) for an initial coherent state located at  $q_0 = 1$  and  $p_0 = 0$  for a strong damping regime  $\gamma = 0.5$ , and the zero-temperature (left) and finite-temperature (right) environmental models. The form of the Gaussian packet is shown at different times of the evolution: (a)  $\tau = 0$ , (b)  $\tau = \pi/4\nu$ , (c)  $\tau = \pi/2\nu$ , (d)  $\tau = 3\pi/4\nu$ , and (e)  $\tau = \pi/\nu$ . The modulation parameters are  $\lambda = 0.5$  and  $\nu = 0.1$ .

the derivation of the analytical solutions was given without specifying the driving forces or initial conditions. The first type of driving studied was a generalization of the forced oscillator which encompasses also the classical pumping of

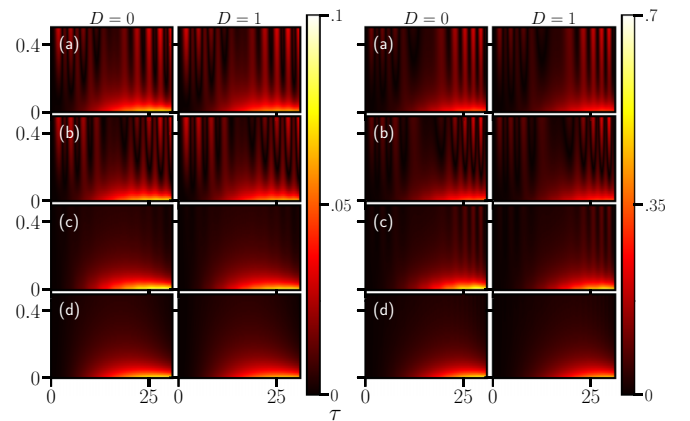


FIG. 9. Relative error of rows (a), the standard deviation of position  $\delta\sigma_x = \delta\sqrt{\langle \hat{x}^2 \rangle - \langle \hat{x} \rangle^2}$ ; rows (b), the standard deviation of momentum  $\delta\sigma_p = \delta\sqrt{\langle \hat{p}^2 \rangle - \langle \hat{p} \rangle^2}$ ; rows (c), the energy; and rows (d), the uncertainty relation  $\delta\sigma_x\sigma_p$ . The errors for modulation amplitudes of  $\lambda = 0.1$  and  $\lambda = 0.5$  are shown on the left and right, respectively. The vertical axis corresponds to the values of the damping parameter  $\gamma$  varying from 0.01 to 0.5 and the horizontal axis is the time evolution of the system for the initial time  $\tau = 0$  to roughly half the period of the modulation  $\tau = \pi/\nu$ .

a radiation mode model. In this type of driving, resonances disappear in the classical pumping type of driving since an equilibrated rate of population and depopulation of energy states happens. On the other hand, whenever the rate of population and depopulation is not balanced, resonances appear. It was additionally observed that the effects of the driving and the effects of the thermalization (diffusion of the wave packet) are decoupled, in the sense that the drive has no influence on the form of the Gaussian state, and its effect is only noticed in the trajectories of the Gaussian state in the phase space. This is at a certain point what one would expect since the range of energies needed to generate the diffusion of the wave packet is much smaller and delocalized than the energy provided by the driving. Finally, the appearance of dense trajectories in the long-time limit indicates the emergence a nonequilibrium stationary condition at which the rate of dissipation is compensated by the gain or loss of energy due to the driving. The second type of driving considered here was obtained from the coupling of the oscillator with an additional two-level system, whose interaction is time dependent. The reduced dynamics was studied for both systems and in the case of the oscillator, the driving appearing due to the time-varying coupling has exactly the same form as the generalized forced type of driving studied in the first part, with the difference that the oscillator splits into a mixture of two Gaussian states following opposite directions. The purity of the oscillator depends on the distance between the two Gaussian states. On the other hand, the influence of the time-varying coupling on the qubit has an effect only on the nondiagonal element due to the type of coupling considered here (dephasing). For the nondiagonal element we saw an important gain of coherence in the qubit, when the driving produces equilibrated rates of gain and loss of energy states. The last type of driving explored is due to a modulation of the angular frequency of the oscillator which has the effect to shrink or stretch the harmonic potential or equivalently to increase or decrease the energy level spacing. For this type of system, an analytical solution was derived under the adiabatic approximation for which a fundamental matrix (which is the key point in obtaining an analytical solution) can be obtained in a closed form. For this type of driving, the first and second moments of the oscillator are affected due to the adiabatic modulation of the frequency, unlike the previous types of driving whose action on the dynamics is only to drive the system through different regions in the phase space. In particular, the case of a harmonic modulation has been explored under the adiabatic limit, where deformation of the trajectories and a wiggling of the energy profile were observed due to the periodic flattening and squashing of the potential. Furthermore, due to the modulation, an initial Gaussian state in its transition to the stationary condition due to the interaction with the environment is periodically deformed into a squeezed shape. The error intrinsic in the solution due to the adiabatic assumptions was also briefly discussed and it was found that this encounters a maximum value at times which depend on the modulation parameters. It must be taken into account that the errors carried in the second moments may appear as a violation of the uncertainty principle, although this is not really the case, as this is only a consequence of the adiabatic limit in which the approximations to the dynamics are based.

## ACKNOWLEDGMENTS

The author thanks Professor T. Gorin for enlightening discussions concerning Sec. V of this paper. Also, the hospitality of the Centro Internacional de Ciencias, UNAM, where some of the discussions took place, is gratefully acknowledged.

## APPENDIX A: SOLUTION FOR THE DRIVING DUE TO AN EXTERNAL TIME-DEPENDENT FORCE

In the chord function representation, the master equation is written as

$$\hat{L}w = -i[f(\tau)s - g(\tau)k]w, \quad (\text{A1})$$

where  $w = w(\vec{r}, \tau) = w(k, s, \tau)$ , we have defined  $\gamma_+ = 2\gamma(\bar{n} + 1/2)$ , and  $\hat{L}$  is a linear differential operator of the form

$$\hat{L} = \partial_\tau + (s + \gamma k)\partial_k - (k - \gamma s)\partial_s + \frac{\gamma_+}{2}(k^2 + s^2). \quad (\text{A2})$$

The master equation is now a first-order partial differential equation which can be placed in the form of a set of ordinary parametric differential equations

$$\dot{k} = s + \gamma k, \quad (\text{A3})$$

$$\dot{s} = -k + \gamma s, \quad (\text{A4})$$

$$\dot{w} = -\left( if(\tau)s - ig(\tau)k + \frac{\gamma_+}{2}(k^2 + s^2) \right) w. \quad (\text{A5})$$

Equations (A3) and (A4) can be placed together into a second-order ordinary differential equation of an undamped harmonic oscillator  $\ddot{k} - 2\gamma\dot{k} + \kappa^2 k = 0$ , where  $\kappa^2 = 1 + \gamma^2$  and the solution for  $s(\tau)$  may be obtained through Eq. (A3),  $s = \dot{k} - \gamma k$ . The solutions for  $k$  and  $s$  are therefore

$$k(\tau) = e^{\gamma\tau/2}(a_1 \sin \tau + a_2 \cos \tau), \quad (\text{A6})$$

$$s(\tau) = e^{\gamma\tau/2}(a_1 \cos \tau - a_2 \sin \tau) \quad (\text{A7})$$

and  $a_1$  and  $a_2$  are the integration constants or characteristic curves which remain constant at all times. The evolution matrix  $\mathbf{R}$  (fundamental matrix) associated with this set of ordinary differential equations, i.e.,  $\vec{r}(\tau + \sigma) = \mathbf{R}(\sigma)\vec{r}(\tau)$ , for  $\vec{r} = (k, s)^T$ , has the form

$$\mathbf{R}(\sigma) = e^{\gamma\sigma} \begin{pmatrix} \cos \sigma & \sin \sigma \\ -\sin \sigma & \cos \sigma \end{pmatrix}, \quad (\text{A8})$$

which represents a contracting-expanding and rotatory map. The matrix  $\mathbf{R}$  is invertible, i.e.,  $\mathbf{R}^{-1}(\tau) = \mathbf{R}(-\tau)$ , possesses group properties  $\mathbf{R}(\tau)\mathbf{R}(\tau') = \mathbf{R}(\tau + \tau')$ , and is independent of the angular frequency  $\kappa$ . The solution of the master equation will be finally obtained by integrating Eq. (A5),

$$\int_{w(\tau)}^{w(\tau+\sigma)} \frac{dw}{w} = -i \int_\tau^{\tau+\sigma} d\tau' [f(\tau')s(\tau') - g(\tau')k(\tau')] - \frac{\gamma_+}{2} \int_\tau^{\tau+\sigma} d\tau' [k^2(\tau') + s^2(\tau')], \quad (\text{A9})$$

where  $w(\tau)$  is the chord function at the initial time  $\tau$ , and thus it represents the initial conditions, and  $w(\tau + \sigma)$  is the chord function at the time  $\tau + \sigma$ , and thus it represents the solution

we are interested in obtaining. With the map described by  $\mathbf{R}$ , it is easy to compute the integration of the right-hand side of (A9) since  $k$  and  $s$  at the time  $\tau'$  can be written with the help of the map (A8) as  $\vec{r}(\tau') = \mathbf{R}(\tau' - \tau - \sigma)\vec{r}(\tau + \sigma)$  and now the integration over the variables becomes an integration over the components of the map described by  $\mathbf{R}$ . After performing the integration of (A9), one can write down an explicit expression for the evolution of this chord function matrix element from some initial time  $\tau$  to an arbitrary final time  $\tau + \sigma$ :

$$\begin{aligned} w(\vec{r}, \tau + \sigma) &= w[\mathbf{R}(-\sigma)\vec{r}, \tau] \exp\left(-\frac{\gamma_+}{2}\alpha(\sigma)|\vec{r}|^2 - i\vec{\chi}(\tau + \sigma) \cdot \vec{r}\right). \end{aligned} \quad (\text{A10})$$

Here  $w[\mathbf{R}(-\sigma)\vec{r}, \tau]$  are the initial conditions of the oscillator in the chord function description and whose dependence on the variables  $k$  and  $s$  has been mapped backward in time with the map described by  $\mathbf{R}$ ;  $\alpha(\sigma)$  is given by

$$\alpha(\sigma) = \int_0^\sigma d\tau' [R_{11}^2(-\tau') + R_{12}^2(-\tau')] = \frac{1 - e^{-2\gamma\sigma}}{2\gamma} \quad (\text{A11})$$

and we have defined the vector  $\vec{\chi}(\tau + \sigma) = [\chi_1(\tau + \sigma), \chi_2(\tau + \sigma)]^T$  whose components are given by

$$\begin{aligned} \chi_1(\tau + \sigma) &= \int_0^\sigma d\sigma' f(\tau + \sigma - \sigma') R_{21}(-\sigma') \\ &\quad - \int_0^\sigma d\sigma' g(\tau + \sigma - \sigma') R_{11}(-\sigma'), \end{aligned} \quad (\text{A12})$$

$$\begin{aligned} \chi_2(\tau + \sigma) &= \int_0^\sigma d\sigma' f(\tau + \sigma - \sigma') R_{22}(-\sigma') \\ &\quad - \int_0^\sigma d\sigma' g(\tau + \sigma - \sigma') R_{12}(-\sigma'), \end{aligned} \quad (\text{A13})$$

where  $R_{ij}$  are the components of the matrix  $\mathbf{R}$  given in (A8). Two particular cases must be explicitly written when a harmonic driving is considered. The first one is of an external driving force for which  $f(\tau) = \lambda \cos \nu\tau$  and  $g(\tau) = 0$ . In this case, the components of the vector  $\vec{\chi}(\tau + \sigma)$  take the form

$$\begin{aligned} \chi_1(\tau + \sigma) &= \frac{\lambda e^{-\gamma\sigma}}{2|\Delta_-|^2} \text{Re}[\Delta_- e^{-i\nu\tau - i\sigma}] \\ &\quad + \frac{\lambda e^{-\gamma\sigma}}{2|\Delta_+|^2} \text{Re}[\Delta_+ e^{-i\nu\tau + i\sigma}] \\ &\quad - \frac{\lambda}{|\Delta_+ \Delta_-|^2} \text{Re}[\Delta_+ \Delta_- e^{-i\nu(\tau + \sigma)}], \quad (\text{A14}) \\ \chi_2(\tau + \sigma) &= \frac{\lambda e^{-\gamma\sigma}}{2|\Delta_-|^2} \text{Im}[\Delta_- e^{-i\nu\tau - i\sigma}] \\ &\quad + \frac{\lambda e^{-\gamma\sigma}}{2|\Delta_+|^2} \text{Im}[\Delta_+ e^{-i\nu\tau + i\sigma}] \\ &\quad - \frac{\lambda}{|\Delta_+ \Delta_-|^2} \text{Im}[(\nu + i\gamma)\Delta_+ \Delta_- e^{-i\nu(\tau + \sigma)}], \end{aligned} \quad (\text{A15})$$

where  $\Delta_+ = \nu + 1 - i\gamma$ ,  $\Delta_- = \nu - 1 - i\gamma$ , and  $R_{21}$  and  $R_{22}$  are components of the map  $\mathbf{R}$  given in (A8). The other case

is when the classical pumping type of driving is assumed for which  $f(\tau) = \lambda \cos \nu\tau$  and  $g(\tau) = \lambda \sin \nu\tau$ . In this case the components of the vector  $\vec{\chi}(\tau + \sigma)$  take the form

$$\begin{aligned} \chi_1(\tau + \sigma) &= \frac{\lambda}{\Delta} \{(\nu + 1)[\cos \nu(\tau + \sigma) - e^{-\gamma\sigma} \cos(\sigma - \nu\tau)] \\ &\quad - \gamma[\sin \nu(\tau + \sigma) + e^{-\gamma\sigma} \sin \nu(\sigma - \nu\tau)]\}, \end{aligned} \quad (\text{A16})$$

$$\begin{aligned} \chi_2(\tau + \sigma) &= \frac{\lambda}{\Delta} \{(\nu + 1)[\sin \nu(\tau + \sigma) + e^{-\gamma\sigma} \sin(\sigma - \nu\tau)] \\ &\quad + \gamma[\cos \nu(\tau + \sigma) - e^{-\gamma\sigma} \cos \nu(\sigma - \nu\tau)]\}, \end{aligned} \quad (\text{A17})$$

where now  $\Delta = (\nu + 1)^2 + \gamma^2$ .

## APPENDIX B: DERIVATION OF THE SOLUTION FOR THE NONDIAGONAL ELEMENT $w_{01}$

For the nondiagonal element master equation (26), the parametric form of the partial differential equation is

$$\dot{k} = s + \gamma k + 2f(\tau), \quad (\text{B1})$$

$$\dot{s} = -k + \gamma s + 2g(\tau), \quad (\text{B2})$$

$$\dot{w}_{01} = \left(i\Delta - \frac{\gamma_+}{2}(k^2 + s^2)\right)w_{01} \quad (\text{B3})$$

and as before we can write down a second-order ordinary differential equation for  $k$  by coupling Eqs. (B1) and (B2), yielding

$$\ddot{k} - \beta\dot{k} + \kappa^2 k = h(\tau), \quad (\text{B4})$$

where  $\kappa^2 = 1 + \gamma^2$ ,  $\beta = 2\gamma$ , and

$$h(\tau) = 2\left(\frac{df(\tau)}{d\tau} + g(\tau) - \gamma f(\tau)\right). \quad (\text{B5})$$

Equation (B4) is a second-order nonhomogeneous differential equation, whose solution is the sum of the homogeneous and the particular parts:  $k(\tau) = k_h(\tau) + k_p(\tau)$ . The solution for the homogeneous part  $\ddot{k}_h - \beta\dot{k}_h + \kappa^2 k_h = 0$  is given in (A6) and the solution for the particular part  $\ddot{k}_p - \beta\dot{k}_p + \kappa^2 k_p = h(\tau)$  can be obtained as the convolution of the nonhomogeneous part  $h(\tau)$  with the Green's function  $G(\tau)$ ,  $k_p(\tau) = \int_0^\tau d\tau' G(\tau - \tau')h(\tau')$ , where  $G(\tau) = e^{\gamma\tau} \sin \tau$  is the solution of the propagator equation  $\ddot{G} - \beta\dot{G} + \kappa^2 G = \delta(\tau - \tau')$ ; here the overdot refers to the derivative with respect to  $\tau$ . The full solution of Eq. (B4) may thus be written as

$$\begin{aligned} k(\tau) &= k_h(\tau) + k_p(\tau) \\ &= e^{\gamma\tau}(a_1 \sin \tau + a_2 \cos \tau) + \Lambda_k(\tau), \end{aligned} \quad (\text{B6})$$

where

$$\Lambda_k(\tau) = \int_0^\tau d\tau' e^{\gamma(\tau - \tau')} \sin(\tau - \tau') h(\tau'). \quad (\text{B7})$$

Solving for  $s$  in the first parametric equation (B1) and then plugging in the result for  $k$ , one has, for  $s$ ,

$$\begin{aligned} s(\tau) &= \dot{k} - \gamma k - 2f(\tau) \\ &= e^{\gamma\tau}(-a_1 \cos \tau + a_2 \sin \tau) + \Lambda_s(\tau), \end{aligned} \quad (\text{B8})$$

where  $\Lambda_s(\tau) = \dot{\Lambda}_k(\tau) - \gamma \Lambda_k(\tau) - 2f(\tau)$  or

$$\Lambda_s(\tau) = \int_0^\tau d\tau' e^{\gamma(\tau-\tau')} \cos(\tau - \tau') h(\tau') - 2f(\tau). \quad (\text{B9})$$

Now, if we redefine the variables as

$$k'(\tau) = k(\tau) + \Lambda_k(\tau), \quad (\text{B10})$$

$$s'(\tau) = s(\tau) + \Lambda_s(\tau), \quad (\text{B11})$$

then one can describe a map that moves any point represented by the prime vector  $\vec{r}'(\tau) = [k'(\tau), s'(\tau)]$  at the time  $\tau$  to another point  $\vec{r}'(\tau') = [k'(\tau'), s'(\tau')]$  at the time  $\tau' = \tau + \sigma$  through the same map as described by the matrix  $\mathbf{R}$  given in (A8), that is,  $\vec{r}'(\tau + \sigma) = \mathbf{R}(\sigma)\vec{r}'(\tau)$ , and together with the relation  $\vec{r}(\tau) = \vec{r}'(\tau) - \vec{\Lambda}(\tau)$ , where

$$\vec{\Lambda}(\tau) = \begin{pmatrix} \Lambda_k(\tau) \\ \Lambda_s(\tau) \end{pmatrix}, \quad (\text{B12})$$

one can build the map that describes the motion of any point  $[k(\tau), s(\tau)]$  along the characteristics as

$$\vec{r}(\tau + \sigma) = \mathbf{R}(\sigma)[\vec{r}(\tau) + \vec{\Lambda}(\tau)] - \vec{\Lambda}(\tau + \sigma). \quad (\text{B13})$$

Integration of the third parametric equation (B3) has the form

$$\begin{aligned} \int_{w_{01}(\tau)}^{w_{01}(\tau+\sigma)} \frac{dw_{01}}{w_{01}} &= \int_\tau^{\tau+\sigma} d\tau' \left( i\Delta - \frac{\gamma_+}{2} |\vec{r}'(\tau')|^2 \right) \\ &= i\Delta\sigma - \frac{\gamma_+}{2} \int_\tau^{\tau+\sigma} d\tau' |\vec{r}'(\tau')|^2, \end{aligned} \quad (\text{B14})$$

where  $|\vec{r}'(\tau')|^2 = k^2(\tau') + s^2(\tau')$ . With the map given in (B13), now one can write  $k(\tau')$  and  $s(\tau')$  appearing in the integrand of the right-hand side of (B14) as

$$|\vec{r}'(\tau')|^2 = |\mathbf{R}(\tau' - \tau - \sigma)[\vec{r}(\tau + \sigma) + \vec{\Lambda}(\tau + \sigma)] - \vec{\Lambda}(\tau')|^2. \quad (\text{B15})$$

Thus, in general terms, this integration can be done, yielding a solution in the form of the chord function

$$\begin{aligned} w_{01}(\vec{r}, \tau + \sigma) &= w_{01}[\mathbf{R}(-\sigma)[\vec{r} + \vec{\Lambda}(\tau + \sigma)] - \vec{\Lambda}(\tau), \tau] \\ &\times \exp \left[ i\Delta\sigma - \frac{\gamma_+}{2} [\alpha(\sigma)|\vec{r}|^2 + 2\vec{\zeta}(\tau + \sigma) \cdot \vec{r}] \right] \\ &\times \exp \left[ -\frac{\gamma_+}{2} \Theta(\tau + \sigma) \right], \end{aligned} \quad (\text{B16})$$

where  $\alpha(\sigma)$  is given in (A11),

$$\begin{aligned} \Theta(\tau + \sigma) &= \alpha(\sigma) |\vec{\Lambda}(\tau + \sigma)|^2 + \int_0^\sigma d\sigma' |\Lambda(\tau + \sigma - \sigma')|^2 \\ &\quad - 2\vec{\Lambda}(\tau + \sigma) \cdot \int_0^\sigma d\sigma' \mathbf{R}^T(-\sigma') \vec{\Lambda}(\tau + \sigma - \sigma'), \end{aligned} \quad (\text{B17})$$

and

$$\vec{\zeta}(\tau + \sigma) = \alpha(\sigma) \vec{\Lambda}(\tau + \sigma) - \int_0^\sigma d\sigma' \mathbf{R}^T(-\sigma') \vec{\Lambda}(\tau + \sigma - \sigma'). \quad (\text{B18})$$

The solution given in (29) is a general solution for which the form of the time-dependent couplings  $f(\tau)$  and  $g(\tau)$  need not be specified.

### APPENDIX C: SOLUTION FOR THE ADIABATIC MODULATION

The master equation described in (35) in the chord function representation reads

$$\{\partial_\tau + [\Omega^2(\tau)s + \gamma k] \partial_k - (k - \gamma s) \partial_s\} w = -\frac{\gamma_+}{2} |\vec{r}|^2 w, \quad (\text{C1})$$

thus, it can be placed as a set of ordinary differential equations, i.e.,

$$\dot{k} = \Omega^2(\tau)s + \gamma k, \quad (\text{C2})$$

$$\dot{s} = -k + \gamma s, \quad (\text{C3})$$

$$\dot{w} = -\frac{\gamma_+}{2} (k^2 + s^2) w. \quad (\text{C4})$$

Under the adiabatic limit, one can write a solution for Eqs. (C2) and (C3) as

$$k(\tau) = \Omega(\tau) e^{\gamma\tau} \{a_1 \sin[\omega(\tau)] + a_2 \cos[\omega(\tau)]\}, \quad (\text{C5})$$

$$s(\tau) = e^{\gamma\tau} \{a_1 \cos[\omega(\tau)] - a_2 \sin[\omega(\tau)]\}, \quad (\text{C6})$$

where  $\omega(\tau) = \int_0^\tau d\tau' \Omega(\tau')$ . As before, one can write down the fundamental matrix corresponding to the set of equations (C5) and (C6), i.e.,  $\vec{r}(\tau_2) = \mathbf{M}(\tau_2, \tau_1)\vec{r}(\tau_1)$ , for  $\vec{r} = (k, s)^T$ , in the form

$$\mathbf{M}(\tau_2, \tau_1) = e^{\gamma\delta\tau} \begin{pmatrix} \frac{\Omega(\tau_2)}{\Omega(\tau_1)} \cos[\omega(\delta\tau)] & \Omega(\tau_2) \sin[\omega(\delta\tau)] \\ -\frac{\sin[\omega(\delta\tau)]}{\Omega(\tau_1)} & \cos[\omega(\delta\tau)] \end{pmatrix}, \quad (\text{C7})$$

where  $\delta\tau = \tau_2 - \tau_1$ . The map also satisfies the relations  $\mathbf{M}(\tau_2, \tau_1)\mathbf{M}(\tau_1, \tau_0) = \mathbf{M}(\tau_2, \tau_0)$  and  $\mathbf{M}^{-1}(\tau_1, \tau_0) = \mathbf{M}(\tau_0, \tau_1)$ . Integration of Eq. (C4) can be easily carried with the employment of the fundamental matrix

$$\int_{w(\tau)}^{w(\tau+\sigma)} \frac{dw}{w} = -\frac{\gamma_+}{2} \int_\tau^{\tau+\sigma} d\tau' |\vec{r}'(\tau')|^2, \quad (\text{C8})$$

where in terms of the fundamental matrix given in (C7), the integrand on the right-hand side can be written as  $\vec{r}'(\tau') = \mathbf{M}(\tau', \tau + \sigma)\vec{r}(\tau + \sigma)$ , yielding the solution for the chord function

$$\begin{aligned} w(\vec{r}, \tau + \sigma) &= w[\mathbf{M}^{-1}(\tau + \sigma, \tau)\vec{r}, \tau] \\ &\times \exp \left( -\frac{\gamma_+}{2} \vec{r}^T \boldsymbol{\alpha}(\tau + \sigma) \vec{r} \right), \end{aligned} \quad (\text{C9})$$

where  $w[\mathbf{M}^{-1}(\tau + \sigma, \tau)\vec{r}, \tau]$  are the initial conditions of the oscillator in the chord function representation, whose variable dependence has been mapped to the time  $\tau + \sigma$  according to map described by the fundamental matrix  $\mathbf{M}$ , and the matrix  $\boldsymbol{\alpha}(\tau + \sigma)$  is a symmetric matrix whose components are given by

$$\alpha_{ij}(\tau + \sigma) = \int_\tau^{\tau+\sigma} d\sigma' [\mathbf{M}(\sigma', \tau + \sigma) \mathbf{M}^T(\sigma', \tau + \sigma)]_{ij}.$$

- [1] J. Gemmer, M. Michel, and G. Mahler, *Quantum Thermodynamics: Emergence of Thermodynamic Behavior Within Composite Quantum Systems*, Lecture Notes in Physics Vol. 784 (Springer, Berlin, 2009).
- [2] F. Binder, S. Vinjanampathy, K. Modi, and J. Goold, *Phys. Rev. E* **91**, 032119 (2015).
- [3] N. H. Y. Ng, L. Manánska, C. Cirstoiu, J. Eisert, and S. Wehner, *New J. Phys.* **17**, 085004 (2015).
- [4] S. Vinjanampathy and J. Anders, *Contemp. Phys.* **57**, 545 (2016).
- [5] J. Millen and A. Xuereb, *New J. Phys.* **18**, 011002 (2016).
- [6] J. Goold, M. Huber, A. Riera, L. del Rio, and P. Skrzypczyk, *J. Phys. A: Math. Theor.* **49**, 143001 (2016).
- [7] H. T. Quan, Y.-x. Liu, C. P. Sun, and F. Nori, *Phys. Rev. E* **76**, 031105 (2007).
- [8] R. S. Whitney, *Phys. Rev. Lett.* **112**, 130601 (2014).
- [9] R. Uzdin, A. Levy, and R. Kosloff, *Phys. Rev. X* **5**, 031044 (2015).
- [10] M. Horodecki and J. Oppenheim, *Nat. Commun.* **4**, 2059 (2013).
- [11] M. Esposito, M. A. Ochoa, and M. Galperin, *Phys. Rev. Lett.* **114**, 080602 (2015).
- [12] J. Anders and M. Esposito, *New J. Phys.* **19**, 010201 (2017).
- [13] A. Levy, R. Alicki, and R. Kosloff, *Phys. Rev. E* **85**, 061126 (2012).
- [14] D. Gelbwaser-Klimovsky, R. Alicki, and G. Kurizki, *Phys. Rev. E* **87**, 012140 (2013).
- [15] V. Semin and F. Petruccione, *Phys. Rev. A* **90**, 052112 (2014).
- [16] R. Schmidt, M. F. Carusela, J. P. Pekola, S. Suomela, and J. Ankerhold, *Phys. Rev. B* **91**, 224303 (2015).
- [17] R. Uzdin, A. Levy, and R. Kosloff, *Entropy* **18**, 124 (2016).
- [18] M. Bauer, K. Brandner, and U. Seifert, *Phys. Rev. E* **93**, 042112 (2016).
- [19] T. Dittrich, P. Hänggi, G.-L. Ingold, B. Kramer, G. Schön, and W. Zwerger, *Quantum Transport and Dissipation* (Wiley-VCH, Weinheim, 1998), Chap. 5.
- [20] M. A. Nielsen and I. L. Chuang, *Quantum Computation and Quantum Information: 10th Anniversary Edition*, 10th ed. (Cambridge University Press, New York, 2011).
- [21] O. V. Zhironov and D. L. Shepelyansky, *Phys. Rev. Lett.* **100**, 014101 (2008).
- [22] T. E. Lee and H. R. Sadeghpour, *Phys. Rev. Lett.* **111**, 234101 (2013).
- [23] S. Walter, A. Nunnenkamp, and C. Bruder, *Phys. Rev. Lett.* **112**, 094102 (2014).
- [24] V. Ameri, M. Eghbali-Arani, A. Mari, A. Farace, F. Kheirandish, V. Giovannetti, and R. Fazio, *Phys. Rev. A* **91**, 012301 (2015).
- [25] S. Sonar, M. Hajdušek, M. Mukherjee, R. Fazio, V. Vedral, S. Vinjanampathy, and L.-C. Kwek, *Phys. Rev. Lett.* **120**, 163601 (2018).
- [26] M. P. Silveri, J. A. Tuorila, E. V. Thuneberg, and G. S. Paraoanu, *Rep. Prog. Phys.* **80**, 056002 (2017).
- [27] C. M. Wilson, T. Duty, F. Persson, M. Sandberg, G. Johansson, and P. Delsing, *Phys. Rev. Lett.* **98**, 257003 (2007).
- [28] C. M. Wilson, G. Johansson, T. Duty, F. Persson, M. Sandberg, and P. Delsing, *Phys. Rev. B* **81**, 024520 (2010).
- [29] L. Magazzù, P. Forn-Díaz, R. Belyansky, J.-L. Orgiazzi, M. A. Yurtalan, M. R. Otto, A. Lupascu, C. M. Wilson, and M. Grifoni, *Nat. Commun.* **9**, 1403 (2018).
- [30] J. Piilo and S. Maniscalco, *Phys. Rev. A* **74**, 032303 (2006).
- [31] H. P. Breuer and F. Petruccione, *The Theory of Open Quantum Systems* (Oxford University Press, New York, 2002).
- [32] M. A. Prado Reynoso, P. C. López Vázquez, and T. Gorin, *Phys. Rev. A* **95**, 022118 (2017).
- [33] P. C. L. Vázquez, A. García, and G. Sánchez-González, *Phys. Scr.* **92**, 125101 (2017).
- [34] S. Abdel-Khalek, K. Berrada, and H. Eleuch, *Ann. Phys. (NY)* **361**, 247 (2015).
- [35] A. Wallraff, D. I. Schuster, A. Blais, L. Frunzio, R.-S. Huang, J. Majer, S. Kumar, S. M. Girvin, and R. J. Schoelkopf, *Nature (London)* **431**, 162 (2004).
- [36] I. Chiorescu, P. Bertet, K. Semba, Y. Nakamura, C. J. P. M. Harmans, and J. E. Mooij, *Nature (London)* **431**, 159 (2004).
- [37] Y. Makhlin, G. Schön, and A. Shnirman, *Rev. Mod. Phys.* **73**, 357 (2001).
- [38] A. T. Sornborger, A. N. Cleland, and M. R. Geller, *Phys. Rev. A* **70**, 052315 (2004).
- [39] V. Peano and M. I. Dykman, *New J. Phys.* **16**, 015011 (2014).
- [40] A. M. de Almeida, *Phys. Rep.* **295**, 265 (1998).
- [41] A. M. O. de Almeida, *J. Phys. A: Math. Gen.* **36**, 67 (2003).
- [42] A. B. Klimov and S. M. Chumakov, *A Group-Theoretical Approach to Quantum Optics* (Wiley-VCH, Weinheim, 2009).
- [43] S. He, Y.-Y. Zhang, Q.-H. Chen, X.-Z. Ren, T. Liu, and K.-L. Wang, *Chin. Phys. B* **22**, 064205 (2013).
- [44] J. Q. You and F. Nori, *Nature (London)* **474**, 589 (2011).
- [45] S. M. Girvin, M. H. Devoret, and R. J. Schoelkopf, *Phys. Scr.* **T137**, 014012 (2009).
- [46] A. Caldeira and A. Leggett, *Physica A* **121**, 587 (1983).
- [47] P. C. L. Vázquez and R. Santos-Silva, [arXiv:1801.05943](https://arxiv.org/abs/1801.05943) [quant-ph].
- [48] C. Gerry and P. Knight, *Introductory Quantum Optics* (Cambridge University Press, Cambridge, 2004).
- [49] H. Weyl, *Z. Phys.* **46**, 1 (1927).
- [50] H. Moya-Cessa and M. F. Guasti, *Phys. Lett. A* **311**, 1 (2003).
- [51] S. Mandal, *Opt. Commun.* **386**, 37 (2017).